Materials Today Advances 9 (2021) 100133

Contents lists available at ScienceDirect

Materials Today Advances

journal homepage: www.journals.elsevier.com/materials-today-advances/

Achieving superlubricity with 2D transition metal carbides (MXenes) and MXene/graphene coatings

S. Huang [a], K.C. Mutyala [c, d], A.V. Sumant [c, **], V.N. Mochalin [a, b, *]

[a] Department of Chemistry, Missouri University of Science & Technology, Rolla, MO, 65409, USA
[b] Department of Materials Science & Engineering, Missouri University of Science & Technology, Rolla, MO, 65409, USA
[c] Center for Nanoscale Materials, Argonne National Laboratory, Lemont, IL, 60439, USA
[d] Currently at Ford Motor Company, Dearborn, MI, 48124, USA

ARTICLE INFO

Article history:
Received 16 October 2020
Received in revised form
2 December 2020
Accepted 8 December 2020
Available online 27 February 2021

Keywords:
2D materials
2D transition metal carbides and nitrides
Tribology
Wear
Lubrication

ABSTRACT

Two-dimensional (2D) materials have demonstrated unique friction and antiwear properties unmatched by their bulk (3D) counterparts. A relatively new, large and quickly growing family of two-dimensional early transition metal carbides and nitrides (MXenes) present a great potential in different applications. There is a growing interest in understanding the mechanical and tribological properties of MXenes, however, no report of MXene superlubricity in a solid lubrication process at the macroscale has been presented. Here we investigate the tribological properties of two-dimensional titanium carbide (Ti_3C_2) MXene deposited on SiO_2-coated silicon (Si) substrates subjected to wear by sliding against a diamond-like carbon (DLC)-coated steel ball counterbody using a ball-on-disc tribometer. We have observed that a reduction of the friction coefficient to the superlubric regime (0.0067 ± 0.0017) can be achieved with Ti_3C_2 MXene in dry nitrogen environment. Moreover, the addition of graphene to Ti_3C_2 further reduced the friction by 37.3% and wear by the factor of 2 as compared to Ti_3C_2 alone, while the superlubricity behavior of the MXene remains unchanged. These results open up new possibilities for exploring the family of MXenes in various tribological applications.

© 2021 The Authors. Published by Elsevier Ltd. This is an open access article under the CC BY-NC-ND license (http://creativecommons.org/licenses/by-nc-nd/4.0/).

1. Introduction

Efficiency and life span of machinery, which are affected by friction, lubrication, and wear of materials, become increasingly crucial in modern society [1]. Concerns about the increased consumption of non-renewable energy resources, such as coal and petroleum, demand minimization of friction in transportation and industrial sectors [2]. Thus, the discovery and development of excellent lubricant materials to combat friction and wear are of great importance. Solid 2D lubricants such as graphene [2,3], graphene oxide [4], and molybdenum disulfide (MoS_2) [5] are now gaining much attention for this purpose because of their superior mechanical properties and environmental benignancy compared with oil-based lubricants. Many experimental and theoretical studies have investigated the tribological behavior of 2D materials [6–12]. In particular, graphene has shown outstanding tribological properties as promising lubricant, as well as excellent additive to compositions for wear and friction reduction purposes. The possibility to achieve superlubricity in various atmospheric conditions at the macroscale, utilizing graphene and other 2D materials and their combinations, is another big step [13–16]. MXenes are a new class of two-dimensional early transition metal carbides/nitrides discovered in 2011 [17,18]. MXenes are produced by etching of the A element layers from bulk MAX phases, where 'M′ represents an early transition metal (such as scandium [Sc], yttrium [Y], titanium [Ti], zirconium [Zr], hafnium [Hf], vanadium [V], niobium [Nb], tantalum [Ta], chromium [Cr], molybdenum [Mo], or tungsten [W]), 'A′ is a group IIIA or IVA element (such as aluminum [Al], gallium [Ga], indium [In], silicon [Si], germanium [Ge], etc.), and X can be either carbon (C), nitrogen (N) or both [19]. As a relatively new, large and quickly growing class of 2D materials, MXenes have been studied in various applications, including supercapacitors [20], lasers [21], electromagnetic interference (EMI) shielding and THz communication [22], batteries [23–26], sensors [27–30], etc. Thermal stability [31] and mechanical properties [32,33] of individual MXene flakes have been studied computationally on a large

* Corresponding author.
** Corresponding author.
E-mail addresses: sumant@anl.gov (A.V. Sumant), mochalinv@mst.edu (V.N. Mochalin).

https://doi.org/10.1016/j.mtadv.2021.100133
2590-0498/© 2021 The Authors. Published by Elsevier Ltd. This is an open access article under the CC BY-NC-ND license (http://creativecommons.org/licenses/by-nc-nd/4.0/).

scale, as well as experimentally [34], and their adhesion behavior has also been investigated recently [35,36]. MXenes are promising candidates for tribological applications because of their outstanding mechanical strength and bending rigidity [32,34,37] and a possibility for precise control over the monolayer thickness [38–40]. Yang et al. reported that the addition of 1.0 wt% Ti_3C_2 MXene improved the antifriction properties of base oil [41]. In a similar study published by Zhang et al., 1.0 wt% of 10–20 nm Ti_3C_2 nanosheets effectively improved the friction and antiwear properties of base oil [42]. Liu et al. reported a lower friction coefficient and ball wear volume achieved with 0.8 wt% of highly exfoliated Ti_3C_2 added to base oil [43].

Titanium carbide (Ti_3C_2) MXene is also a promising material for solid lubrication. Zhang et al. reported on the synthesis of Ti_3C_2/ultra-high molecular weight polyethylene composites that reduced the plow friction and adhesive wear [44]. Mai et al. designed Ti_3C_2 nanosheets/copper composites with a 19 times lower wear rate and a 46% reduction in the coefficient of friction (COF) compared to the bare copper counterbody under dry sliding [45]. Recently, Yin et al. created Ti_3C_2/nanodiamond composites that showed the ultrawear resistance when rubbed against a polytetrafluoroethylene (PTFE) ball at room temperature in air. According to the authors, the combination of the rolling action of nanodiamond with the slipping and intercalation of MXene provided the reduction in wear [46]. Hu et al. reported $Ti_3C_2T_x$/Al composites with COF 0.2 in dry sliding test, which is twice lower than that of bare Al [47]. Zhang et al. predicted using modeling that defects, such as Ti and O vacancies in MXene structure, increase the COF through increasing its surface roughness. And compared with the -O- terminated Ti_3C_2, the −OH terminations of Ti_3C_2 further reduced its interlayer COF [48]. Rosenkranz et al. verified that both surface terminations and intercalated water in $Ti_3C_2T_x$ MXene reduced the interfacial bonding strength, resulting in a lower frictional force under dry conditions on stainless steel surfaces [49]. Researchers have also demonstrated that Ti_3C_2 MXene can act as solid lubricant on different substrates at the nanoscale [36,50,51]. All these studies utilizing MXene alone or in combination with other 2D materials have shown that MXenes have great potential as solid lubricants, however, none of these studies reported superlubricity either using MXene itself or in combination with other materials. However, it should be noted that MXenes may be quite reactive towards environment, in particular, water [52–55] and water vapor, as well as other gaseous species [27] may result in MXene degradation or at least, change its surface terminations. Therefore, it becomes important to conduct measurements in an inert atmosphere.

In this work, we investigate the tribological properties of Ti_3C_2 MXene as well as MXene/graphene films on Si substrates coated with thin film of SiO_2 (~300 nm thick SiO_2, from Silicon Valley Microelectronics, hereafter referred to as 'Si substrates') subjected to wear by sliding against a diamond-like carbon (DLC)-coated stainless steel ball using a ball-on-disc tribometer operated in a controlled environment. We demonstrate that it is possible to achieve superlubricity with MXene alone as well as in combination with graphene, with an additional benefit of reduced wear in the latter case.

2. Experimental details

2.1. Preparation of Ti_3C_2 MXene and Ti_3C_2/graphene coatings on Si substrates

Ti_3AlC_2 MAX phase was synthesized by heating a mixture of Ti (−325 mesh, 99.5%, Alfa Aesar), Al (−325 mesh, 99.5%, Alfa Aesar), and graphite (−325 mesh, 99%, Alfa Aesar) powders (3:1.1:1.88 M ratio) at a rate of 10 °C/min from RT to 1550 °C and holding at this temperature for 2 h. Heating and cooling were entirely conducted under argon (Ar) flow. Ti_3C_2 MXene was synthesized according to the published methods [53]. Briefly, the etchant was prepared by adding 0.3 g lithium fluoride (LiF) to 3 mL 9 M HCl in a plastic centrifuge tube and stirring for 5 min. 0.3 g of Ti_3AlC_2 MAX phase powder (−400 mesh, particle size ≤ 38 μm) was gradually added to the etchant and left reacting for 36 h at 35 °C. The etched powder was washed with deionized water until the pH of the supernatant reached ~6. The Ti_3C_2 colloidal solution was then obtained by 5 min hand-shaking followed by 40 min centrifugation at 3500 rpm.

Samples of Ti_3C_2 on Si substrates (average flake size ~0.8 μm, Fig. 1) were produced by 20 min bath sonication of the as-prepared MXene colloidal solution and spray-coated from ~1.5 mL of the diluted as-prepared aqueous colloidal solution (0.017 mg/mL MXene). Ti_3C_2/graphene coatings were prepared by mixing diluted Ti_3C_2 colloidal solution (0.017 mg/mL) and graphene ethanol solution (0.010 mg/mL, Graphene Supermarket, carbon content 99.99%, average flake size ~550 nm) in a 1:1 vol ratio followed by 20 min bath sonication. ~1.5 mL of this dispersion was spray-coated on the Si substrates. All samples were dried in ambient environment for more than 24 h before testing. All Si substrates used in this work were treated overnight in piranha solution (concentrated sulfuric acid: hydrogen peroxide = 3: 1) prior to film deposition.

2.2. Friction and wear tests

Friction and wear tests were conducted in dry nitrogen atmosphere (Dew Point Temperature −40 °C, ≤ RH 0.1%) at room temperature using a multifunctional ball-on-disc type tribometer (MFT-5000, Rtec Instruments). The Si substrates with deposited films were clamped on a sample platform and slid against a 9.526 mm diameter stainless steel ball coated with diamond-like carbon (DLC) film as described elsewhere [56,57]. The applied normal load was controlled at 2 N (maximum contact pressure 0.60 GPa) with 0.1 m/s linear velocity for a total running time of 1 h. Zero calibration of the machine was carried out automatically before each test.

2.3. Characterization

Raman spectroscopy was performed using Renishaw InVia confocal Ramanspectrometer with 532 nm laser, 100x objective and a 1200 l/mm grating. The spectra were acquired with 500 s exposure time, 0.5% of laser power and 1 accumulation.

Atomic force microscopy (AFM) was performed using Digital Instruments Nanoscope IIIA under ambient atmosphere. The AFM image of Ti_3C_2 was recorded in tapping mode with a silicon tip (App Nano, Tip radius < 10 nm).

3. Results and discussion

3.1. Tribological behavior of MXene coating

Friction tests were first conducted on the Si substrates vs. DLC-coated balls for comparison. The experimental COFs for a Si substrate and Ti_3C_2 MXene against the DLC-coated ball are shown in Fig. 2 where the dash-dotted line represents the superlubric threshold (COF = 0.01). The average measured COF for Si substrate against DLC in the range 700–1800 s (before the failure point) is 0.0222 ± 0.0035, whereas the average COF for Ti_3C_2 against DLC in the range 700–3100 s, i.e. before the failure point, is in the superlubricity range, 0.0067 ± 0.0017, as shown in Fig. 2(b). The COF value for Ti_3C_2 is 3.3 times lower than for the Si substrate. Failure points at ~1800 s and 3100 s for the Si substrate and Ti_3C_2 coating,

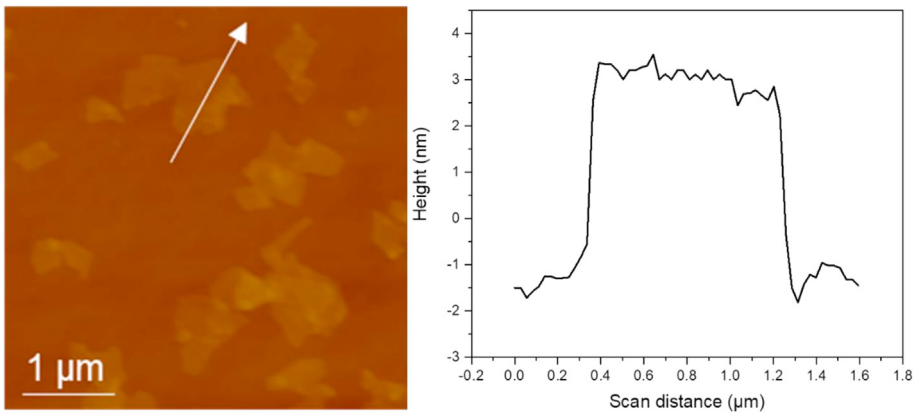

Fig. 1. AFM image (left) and height profile (right) of Ti_3C_2 coatings on Si substrate measured along the white arrow indicated in the left panel.

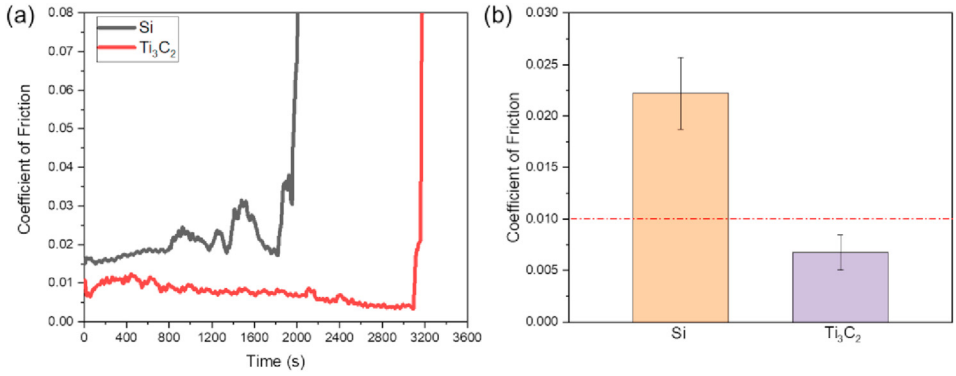

Fig. 2. (a) Tribological behavior of Si substrate and Ti_3C_2 on Si substrate against a DLC-coated steel ball and; (b) comparison of COF values demonstrating the onset of superlubricity. Error bars represent standard deviations of the average COF values.

respectively (Fig. 2(a)), are due to wearing out of DLC coating on the ball as explained below based on the wear marks observed on the counterbody after wear tests.

X-ray photoelectron spectroscopy (XPS) data for similar MXene samples published before [22,35] showed the presence of Ti, C, O, F, and Cl elements, indicating that our MXenes are terminated with different functional groups (T = −OH, −F, -O- and -Cl), in good agreement with other literature data [58]. As hypothesized in prior studies, the surface terminations may affect friction by changing the interlayer binding/adhesion energy of MXenes resulting in a lower COF [49,59]. However, in this case, we believe that the inert nature of the DLC counterbody as well as graphene-like shearing of MXene flakes were mostly responsible for reducing the friction to superlubric regime. Since we did not passivate MXene, it may react over time of the experiment, which may eventually degrade the 2D nature of the MXene. When this happens, shearing becomes disturbed, leading to high friction that wears down DLC and results in a rapid increase of friction to very high values towards the end of the tribo tests as shown in Fig. 2(a). Optical microscopy images of the wear tracks for the Si substrate and Ti_3C_2 samples are shown in Fig. 3(a and b). Raman spectroscopy was further conducted on the wear tracks of the samples. Fig. 3(c and d) show Raman spectra recorded from the wear tracks on the Si substrate and Ti_3C_2 coatings, respectively. Only Si peaks at 300, 520, and ~960 cm^{-1} were observed in four representative spots on Si substrate (Fig. 3(c)) [60]. The Ti_3C_2 sample showed superlubric COF after 700 s and high friction after 3100 s when DLC coating has worn out exposing the underlying steel on the counterbody surface (Fig. 2(a)). Raman spectra show only crystalline and amorphous Si peaks for spots 2–4 within the wear track (Fig. 3(d)) and no signs of MXene. Fig. 3(e and f) show the optical microscopy images of the balls worn against the Si substrate and Ti_3C_2, respectively. The DLC coatings were worn out in both tests on the Si substrate and Ti_3C_2 samples, clearly exposing the underlying steel surface of the balls. Although in case of Ti_3C_2 superlubricity was achieved, the wear was still high. This could be due to a relatively sparse coverage , exposing Si in gaps between the flakes, as shown in AFM image (Fig. 1), which leads to the intermittent contact between Si and DLC, thus increasing the overall wear. However, this did not affect COF on average since the flakes shear easily and are mobile within the wear track, thus despite the sparse nature of the coating, Ti_3C_2 maintained low friction over a period of time. This behavior is similar to that of graphene flakes observed previously on steel surfaces [2].

3.2. Tribological behavior of MXene/graphene coating

From the experiments described above, Ti_3C_2 reaches the superlubic regime but the coating is worn out finally. To check if it is possible to maintain superlubricity and reduce wear of the counterbody even further, we have also tried to fabricate a composite MXene-graphene coating prepared from mixing solution-processed graphene with Ti_3C_2 using sonication. A similar strategy, when MXene was combined with another 2D material, was shown to improve mechanical properties of the resulting composite [61]. Another benefit of adding graphene to MXene coating is to protect MXene from the effects of the environment, since the hydrophobic nature of graphene may reduce exposure of MXene to humidity that is detrimental to its structure [52,53]. A recent high-

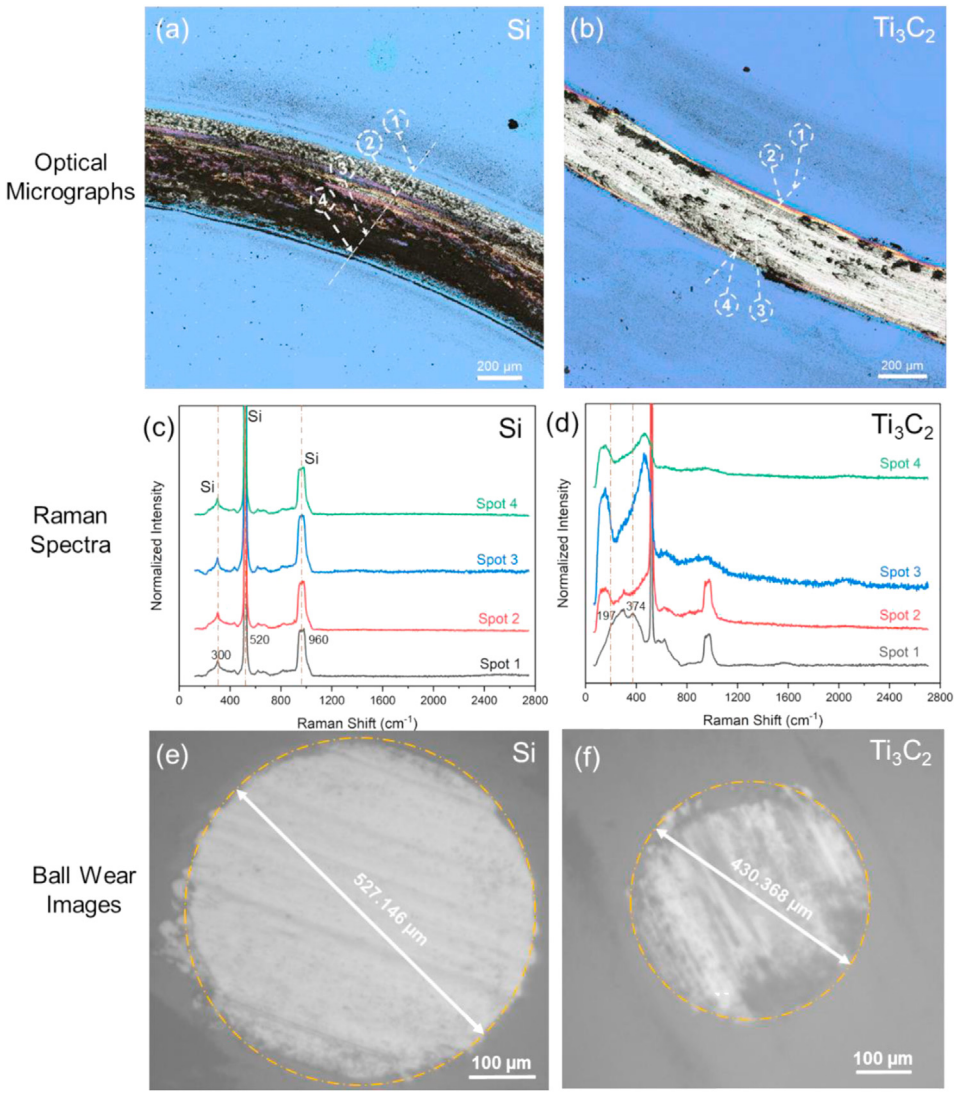

Fig. 3. Top row: optical microscopy images of the wear tracks on (a) Si substrate and (b) Ti_3C_2 samples; middle row: Raman spectra from representative spots on (c) Si substrate and (d) Ti_3C_2 samples; bottom row: optical microscopy images of the balls worn against (e) Si substrate and (f) Ti_3C_2 samples.

resolution microscopy study [62] also showed that the introduction of graphene nanosheets may induce the formation of the lubricating tribofilm protecting the contact surface. Fig. 4(a and b) display the friction test results of graphene, Ti_3C_2, and Ti_3C_2/graphene coatings, respectively, on Si substrates tested against DLC. The average friction coefficient for graphene vs. DLC was 0.0138 ± 0.0014 (700–3600 s), while for the Ti_3C_2/graphene (~37 wt% of graphene) coating, it was reduced to 0.0042 ± 0.0011

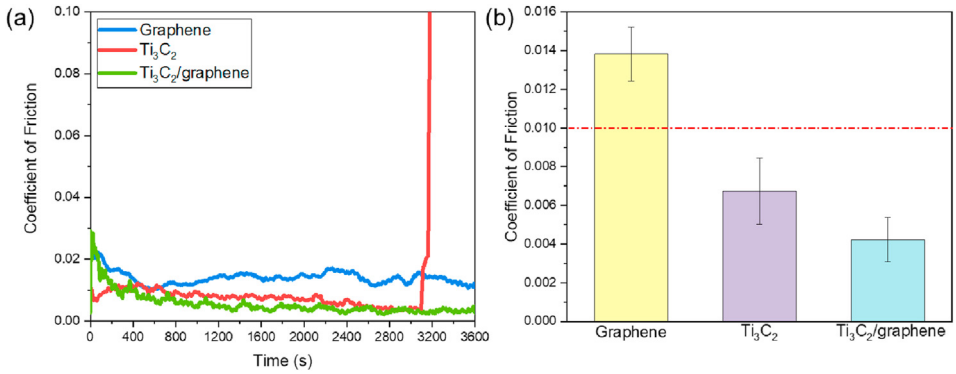

Fig. 4. (a) Tribological behavior of graphene, Ti_3C_2, and Ti_3C_2/graphene coatings against DLC-coated steel balls and (b) comparison of the corresponding COF values. Error bars represent standard deviations of average COF values.

(700−3600 s), which not only reached the superlubricity range but indeed reduced the wear of the DLC ball significantly. The lower friction coefficient of Ti_3C_2/graphene vs. DLC could be attributed to the additional shearing and covering of MXene by graphene during the sliding process thereby reducing wear on the DLC side. It is also possible that graphene may have helped in passivating the reactive surface of MXene during friction. However, while the addition of 37 wt% graphene to MXene reduced the COF from 0.0067 ± 0.0017 to 0.0042 ± 0.0011, a 100 wt% graphene coating yielded a higher COF of 0.0138 ± 0.0014 indicating that a balance between graphene and MXene concentrations must be maintained to achieve the best performance. Thus, we experimentally demonstrated that a combination of Ti_3C_2 MXene with a certain amount of graphene provides the lowest friction coefficient and lower wear than Ti_3C_2 alone.

Optical microscopy images and Raman spectra of the wear track on graphene-coated Si substrate are shown in Fig. 5(a, c), respectively. Raman signature of graphene is observed in spots 1, 2, and 4 in Fig. 5(c) with an increasing intensity of D band, indicating progressive amorphization when moving from the edges to the center of the wear track. The Raman spectrum from spot 3 shows amorphous carbon, which might be part of the transfer layer from DLC coating of the counterbody. Compared with Ti_3C_2 (Fig. 3(b)), the wear track on Ti_3C_2/graphene coating vs. DLC after the test appears to be less abrasive (Fig. 5(b)). Raman spectra from the wear track on Ti_3C_2/graphene sample showed amorphous carbon originating either from graphene remaining in the track or from DLC coating on the ball. In case of graphene, the wear is smaller according to Raman results (Fig. 5) and friction test (Fig. 4). Neat graphene film has more complete coverage and therefore friction interface is mostly between DLC and graphene and not with the underlaying SiO_2, resulting in a lower wear rate of the DLC ball. In case of Ti_3C_2/graphene, the coverage is sparser as can be deduced indirectly by looking at the intensity of the SiO_2 peak in the Raman spectra of the wear track (Fig. 5(d)) and comparing it with the Raman spectra shown in Fig. 5(c). The higher intensity of SiO_2 peak in case of Ti_3C_2/graphene indicates that more SiO_2 is exposed and therefore the friction interface is mixed, increasing the likelihood of the intermittent contact between DLC and SiO_2. Although the overall friction is still dominated by DLC-Ti_3C_2 contact (hence the superlubricity is unchanged), a higher contribution from the intermittent contact with the SiO_2 must be responsible for the higher wear rate.

Images of the wear scars on the counterbody were also analyzed. For graphene and Ti_3C_2/graphene-coated samples, relatively small wear scars were observed after the tests (Fig. 5(e and f)). The ball wear volume was estimated using the equation:

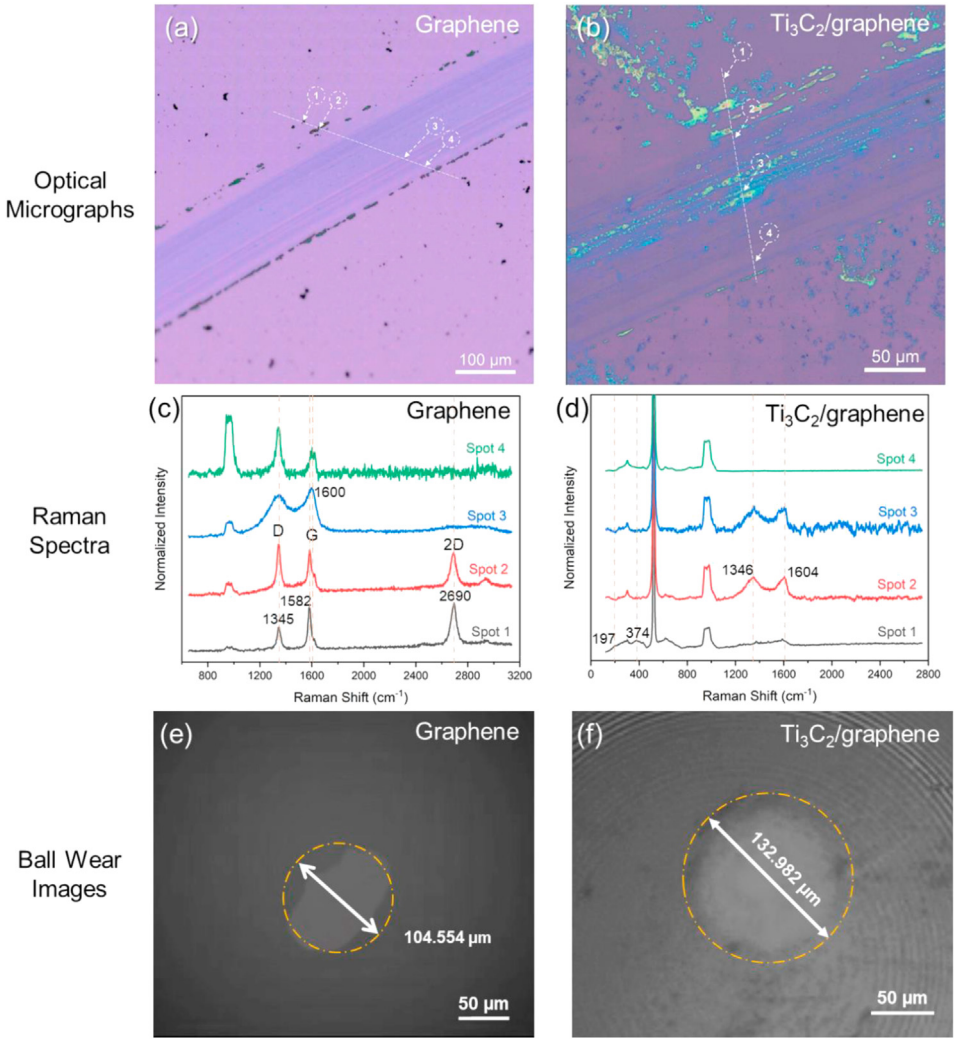

Fig. 5. Top row: optical microscopy images of the wear tracks on (a) graphene and (b) Ti_3C_2/graphene coatings; middle row: Raman spectra from representative spots for (c) graphene and (d) Ti_3C_2/graphene samples; bottom row: optical microscopy images of the balls worn against (e) graphene, and (f) Ti_3C_2/graphene samples.

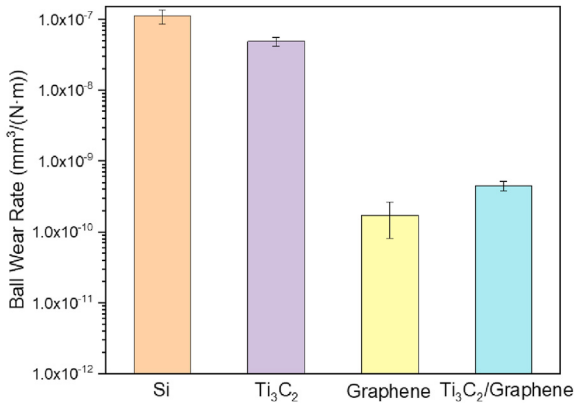

Fig. 6. Ball wear rate against Si substrate, Ti_3C_2, graphene, and Ti_3C_2/graphene coated Si substrates.

$$V = \left(\frac{\pi h}{6}\right)\left(\frac{3d^2}{4} + h^2\right) \quad (1)$$

where

$$h = r - \sqrt{r^2 - d^2/4} \quad (2)$$

d is the diameter of the ball wear cap, and r is the radius of the DLC-coated ball (4.763 mm).

The ball wear rate was estimated using Archard's equation [63,64]:

$$K_B = \frac{V}{SW} \quad (3)$$

where V is the ball wear volume, S is the sliding distance (360 m in our study), and W is the applied load.

The ball wear rates against the Si substrate, Ti_3C_2, graphene, and Ti_3C_2/graphene coatings are summarized in Fig. 6. The Si substrate showed the largest wear rate as expected. Although achieving superlubricity, Ti_3C_2 MXene also showed a high wear rate (4.9×10^{-7} $mm^3/(N \cdot m)$). It is worth noting that after adding 37 wt% of graphene, the wear rate of Ti_3C_2 was reduced by a factor of 2, to 4.5×10^{-9} $mm^3/(N \cdot m)$, with COF further reduced by 37.3%. Thus, graphene prolonged the running time of Ti_3C_2 in the friction tests by reducing abrasion while the superlubricity of MXene remained unchanged.

4. Conclusions

In summary, the tribological properties of Ti_3C_2 MXene coatings on Si substrates have been investigated in a controlled environment. The ball-on-disk friction tests were conducted against the DLC-coated steel ball counterbody in dry nitrogen atmosphere and the results show that the average measured COF for Ti_3C_2 is 0.0067 ± 0.0017, falling into the superlubricity range. This COF value is 3.3 times lower than that for the Si substrate. Moreover, with the introduction of 37 wt% graphene to Ti_3C_2, the COF was further reduced by 37.3% (to 0.0042 ± 0.0011) compared with Ti_3C_2, while the ball wear rate of Ti_3C_2 was reduced by a factor of 2. Thus, superlubricity against DLC can be achieved with MXene, furthermore, with the addition of graphene to MXene, the superlubricity of the coating remained unchanged while abrasion was further reduced. This work opens opportunities for exploring the potential of MXenes and MXene/graphene coatings as novel solid lubricants for various applications.

CRediT authorship contribution statement

Shuohan Huang: Conceptualization, Investigation, Formal analysis, Validation, Writing - original draft. **Kalyan C. Mutyala**: Conceptualization, Investigation, Supervision, Writing - review & editing. **Anirudha V. Sumant**: Conceptualization, Supervision, Resources, Project administration, Funding acquisition, Writing - review & editing. **Vadym N. Mochalin**: Conceptualization, Supervision, Resources, Project administration, Funding acquisition, Writing - review & editing.

Data availability statement

The raw/processed data required to reproduce these findings cannot be shared at this time due to technical or time limitations.

Declaration of competing interest

The authors declare that they have no known competing financial interests or personal relationships that could have appeared to influence the work reported in this paper.

Acknowledgments

The authors acknowledge access to the Center for Nanoscale Materials, an Office of Science user facility. This work was supported by the U.S. Department of Energy, Office of Science, Office of Basic Energy Sciences, under Contract No. DE-AC02-06CH11357. Part of this work was supported by the National Science Foundation under Grant No. 1930881 CMMI.

References

[1] K. Holmberg, A. Erdemir, Influence of tribology on global energy consumption, costs and emissions, Friction 5 (2017) 263–284.
[2] D. Berman, A. Erdemir, A.V. Sumant, Graphene: a new emerging lubricant, Mater. Today 17 (2014) 31–42.
[3] X. Zeng, Y. Peng, H. Lang, A novel approach to decrease friction of graphene, Carbon 118 (2017) 233–240.
[4] H. Liang, Y. Bu, J. Zhang, Z. Cao, A. Liang, Graphene oxide film as solid lubricant, ACS Appl. Mater. Interfaces 5 (2013) 6369–6375.
[5] C. Donnet, J. Martin, T. Le Mogne, M. Belin, Super-low friction of MoS_2 coatings in various environments, Tribol. Int. 29 (1996) 123–128.
[6] W. Guo, J. Yin, H. Qiu, Y. Guo, H. Wu, M. Xue, Friction of low-dimensional nanomaterial systems, Friction 2 (2014) 209–225.
[7] O. Penkov, H.J. Kim, H.J. Kim, D.E. Kim, Tribology of graphene: a review, Int. J. Precis. Eng. Manuf. 15 (2014) 577–585.
[8] J. Lin, L. Wang, G. Chen, Modification of graphene platelets and their tribological properties as a lubricant additive, Tribol. Lett. 41 (2011) 209–215.
[9] S.S. Kandanur, M.A. Rafiee, F. Yavari, M. Schrameyer, Z.-Z. Yu, T.A. Blanchet, N. Koratkar, Suppression of wear in graphene polymer composites, Carbon 50 (2012) 3178–3183.
[10] P. Zhu, R. Li, Study of nanoscale friction behaviors of graphene on gold substrates using molecular dynamics, Nanoscale Res. Lett. 13 (2018) 34.
[11] P.C. Uzoma, H. Hu, M. Khadem, O.V. Penkov, Tribology of 2D nanomaterials: a review, Coatings 10 (2020) 897.
[12] A. Rosenkranz, Y. Liu, L. Yang, L. Chen, 2D nano-materials beyond graphene: from synthesis to tribological studies, Appl. Nanosci. 10 (2020) 3353–3388.
[13] D. Berman, S.A. Deshmukh, S.K. Sankaranarayanan, A. Erdemir, A.V. Sumant, Macroscale superlubricity enabled by graphene nanoscroll formation, Science 348 (2015) 1118–1122.
[14] D. Berman, B. Narayanan, M.J. Cherukara, S.K. Sankaranarayanan, A. Erdemir, A. Zinovev, A.V. Sumant, Operando tribochemical formation of onion-like-carbon leads to macroscale superlubricity, Nat. Commun. 9 (2018) 1–9.
[15] D. Berman, A. Erdemir, A.V. Sumant, Approaches for achieving superlubricity in two-dimensional materials, ACS Nano 12 (2018) 2122–2137.
[16] D. Berman, K.C. Mutyala, S. Srinivasan, S.K. Sankaranarayanan, A. Erdemir, E.V. Shevchenko, A.V. Sumant, Iron-nanoparticle driven tribochemistry leading to superlubric sliding interfaces, Adv. Mater. Interfaces 6 (2019) 1901416.

[17] M. Naguib, M. Kurtoglu, V. Presser, J. Lu, J. Niu, M. Heon, L. Hultman, Y. Gogotsi, M.W. Barsoum, Two-dimensional nanocrystals produced by exfoliation of Ti_3AlC_2, Adv. Mater. 23 (2011) 4248–4253.
[18] M. Naguib, V.N. Mochalin, M.W. Barsoum, Y. Gogotsi, 25th anniversary article: MXenes: a new family of two-dimensional materials, Adv. Mater. 26 (2014) 992–1005.
[19] M. Naguib, O. Mashtalir, J. Carle, V. Presser, J. Lu, L. Hultman, Y. Gogotsi, M.W. Barsoum, Two-dimensional transition metal carbides, ACS Nano 6 (2012) 1322–1331.
[20] M. Ghidiu, M.R. Lukatskaya, M.Q. Zhao, Y. Gogotsi, M.W. Barsoum, Conductive two-dimensional titanium carbide 'clay' with high volumetric capacitance, Nature 516 (2014) 78–81.
[21] J. Yi, L. Du, J. Li, L. Yang, L. Hu, S. Huang, Y. Dong, L. Miao, S. Wen, V.N. Mochalin, Unleashing the potential of Ti_2CT_x MXene as a pulse modulator for mid-infrared fiber lasers, 2D Mater. 6 (2019), 045038.
[22] G. Li, N. Amer, H. Hafez, S. Huang, D. Turchinovich, V.N. Mochalin, F.A. Hegmann, L.V. Titova, Dynamical control over terahertz electromagnetic interference shielding with 2D $Ti_3C_2T_y$ MXene by ultrafast optical pulses, Nano Lett. 20 (2019) 636–643.
[23] M. Naguib, J. Halim, J. Lu, K.M. Cook, L. Hultman, Y. Gogotsi, M.W. Barsoum, New two-dimensional niobium and vanadium carbides as promising materials for Li-ion batteries, J. Am. Chem. Soc. 135 (2013) 15966–15969.
[24] Y. Xie, M. Naguib, V.N. Mochalin, M.W. Barsoum, Y. Gogotsi, X. Yu, K.-W. Nam, X.-Q. Yang, A.I. Kolesnikov, P.R. Kent, Role of surface structure on Li-ion energy storage capacity of two-dimensional transition-metal carbides, J. Am. Chem. Soc. 136 (2014) 6385–6394.
[25] J. Jiang, W. Yang, H. Wang, Y. Zhao, J. Guo, J. Zhao, M. Beidaghi, L. Gao, Electrochemical performances of MoO_2/C nanocomposite for sodium ion storage: an insight into rate dependent charge/discharge mechanism, Electrochim. Acta 240 (2017) 379–387.
[26] A. VahidMohammadi, A. Hadjikhani, S. Shahbazmohamadi, M. Beidaghi, Two-dimensional vanadium carbide (MXene) as a high-capacity cathode material for rechargeable aluminum batteries, ACS Nano 11 (2017) 11135–11144.
[27] S. Chertopalov, V.N. Mochalin, Environment-sensitive photoresponse of spontaneously partially oxidized Ti_3C_2 MXene thin films, ACS Nano 12 (2018) 6109–6116.
[28] Y. Guo, M. Zhong, Z. Fang, P. Wan, G. Yu, A wearable transient pressure sensor made with MXene nanosheets for sensitive broad-range human-machine interfacing, Nano Lett. 19 (2019) 1143–1150.
[29] M. Mojtabavi, A. VahidMohammadi, W. Liang, M. Beidaghi, M. Wanunu, Single-molecule sensing using nanopores in two-dimensional transition metal carbide (MXene) membranes, ACS Nano 13 (2019) 3042–3053.
[30] E. Lee, A. VahidMohammadi, Y.S. Yoon, M. Beidaghi, D.-J. Kim, Two-dimensional vanadium carbide MXene for gas sensors with ultrahigh sensitivity toward nonpolar gases, ACS Sens. 4 (2019) 1603–1611.
[31] V. Borysiuk, V.N. Mochalin, Thermal stability of two-dimensional titanium carbides $Ti_{n+1}C_n$ (MXenes) from classical molecular dynamics simulations, MRS commun 9 (2019) 203–208.
[32] V.N. Borysiuk, V.N. Mochalin, Y. Gogotsi, Molecular dynamic study of the mechanical properties of two-dimensional titanium carbides $Ti_{n+1}C_n$ (MXenes), Nanotechnology 26 (2015) 265705.
[33] G. Plummer, B. Anasori, Y. Gogotsi, G.J. Tucker, Nanoindentation of monolayer $Ti_{n+1}C_nT_x$ MXenes via atomistic simulations: the role of composition and defects on strength, Comput. Mater. Sci. 157 (2019) 168–174.
[34] A. Lipatov, H. Lu, M. Alhabeb, B. Anasori, A. Gruverman, Y. Gogotsi, A. Sinitskii, Elastic properties of 2D $Ti_3C_2T_x$ MXene monolayers and bilayers, Sci. Adv. 4 (2018), eaat0491.
[35] Y. Li, S. Huang, C. Wei, C. Wu, V.N. Mochalin, Adhesion of two-dimensional titanium carbides (MXenes) and graphene to silicon, Nat. Commun. 10 (2019) 1–8.
[36] Y. Guo, X. Zhou, D. Wang, X. Xu, Q. Xu, Nanomechanical properties of Ti_3C_2 Mxene, Langmuir 35 (2019) 14481–14485.
[37] V.N. Borysiuk, V.N. Mochalin, Y. Gogotsi, Bending rigidity of two-dimensional titanium carbide (MXene) nanoribbons: a molecular dynamics study, Comput. Mater. Sci. 143 (2018) 418–424.
[38] Y. Dong, S. Chertopalov, K. Maleski, B. Anasori, L. Hu, S. Bhattacharya, A.M. Rao, Y. Gogotsi, V.N. Mochalin, R. Podila, Saturable absorption in 2D Ti_3C_2 MXene thin films for passive photonic diodes, Adv. Mater. 30 (2018) 1705714.
[39] C. Li, S. Kota, C. Hu, M. Barsoum, On the synthesis of low-cost, titanium-based MXenes, J. Ceram. Sci. Technol 7 (2016) 301–306.
[40] P. Collini, S. Kota, A.D. Dillon, M.W. Barsoum, A.T. Fafarman, Electrophoretic deposition of two-dimensional titanium carbide (MXene) thick films, J. Electrochem. Soc. 164 (2017) D573–D580.
[41] J. Yang, B. Chen, H. Song, H. Tang, C. Li, Synthesis, characterization, and tribological properties of two-dimensional Ti_3C_2, Cryst. Res. Technol. 49 (2014) 926–932.
[42] X. Zhang, M. Xue, X. Yang, Z. Wang, G. Luo, Z. Huang, X. Sui, C. Li, Preparation and tribological properties of $Ti_3C_2(OH)_2$ nanosheets as additives in base oil, RSC Adv. 5 (2015) 2762–2767.
[43] Y. Liu, X. Zhang, S. Dong, Z. Ye, Y. Wei, Synthesis and tribological property of $Ti_3C_2T_x$ nanosheets, J. Mater. Sci. 52 (2017) 2200–2209.
[44] H. Zhang, L. Wang, Q. Chen, P. Li, A. Zhou, X. Cao, Q. Hu, Preparation, mechanical and anti-friction performance of MXene/polymer composites, Mater. Des. 92 (2016) 682–689.
[45] Y.J. Mai, Y.G. Li, S.L. Li, L.Y. Zhang, C.S. Liu, X.H. Jie, Self-lubricating Ti_3C_2 nanosheets/copper composite coatings, J. Alloys Compd. 770 (2019) 1–5.
[46] X. Yin, J. Jin, X. Chen, A. Rosenkranz, J. Luo, Ultra-wear-resistant MXene-based composite coating via in situ formed nanostructured tribofilm, ACS Appl. Mater. Interfaces 11 (2019) 32569–32576.
[47] J. Hu, S. Li, J. Zhang, Q. Chang, W. Yu, Y. Zhou, Mechanical properties and frictional resistance of Al composites reinforced with $Ti_3C_2T_x$ MXene, Chin. Chem. Lett. 31 (2019) 996–999.
[48] D. Zhang, M. Ashton, R.G. Hennig, S.B. Sinnott, D. Zhang, A. Ostadhossein, D.A.C.T. van, Computational study of low interlayer friction in $Ti_{n+1}C_n$ (n = 1, 2, and 3) MXene, ACS Appl. Mater. Interfaces 9 (2017) 34467–34479.
[49] A. Rosenkranz, P.G. Grutzmacher, R. Espinoza, V.M. Fuenzalida, E. Blanco, N. Escalona, F.J. Gracia, R. Villarroel, L. Guo, R. Kang, F. Mucklich, S. Suarez, Z. Zhang, Multi-layer $Ti_3C_2T_x$-nanoparticles (MXenes) as solid lubricants - role of surface terminations and intercalated water, Appl. Surf. Sci. 494 (2019) 13–21.
[50] A. Rodriguez, M. Jaman, O. Acikgoz, B. Wang, J. Yu, P. Grutzmacher, A. Rosenkranz, M. Baykara, The potential of Ti_3C_2 nano-sheets (MXenes) for nanoscale solid lubrication revealed by friction force microscopy, Appl. Surf. Sci. 535 (2020) 147664.
[51] X. Zhou, Y. Guo, D. Wang, Q. Xu, Nano friction and adhesion properties on Ti3C2 and Nb2C MXene studied by AFM, Tribol. Int. 153 (2021) 106646.
[52] S. Huang, V.N. Mochalin, Understanding chemistry of two-dimensional transition metal carbides and carbonitrides (MXenes) with gas analysis, ACS Nano 14 (2020) 10251–10257.
[53] S. Huang, V.N. Mochalin, Hydrolysis of 2D transition-metal carbides (MXenes) in colloidal solutions, Inorg. Chem. 58 (2019) 1958–1966.
[54] X. Zhao, A. Vashisth, J.W. Blivin, Z. Tan, D.E. Holta, V. Kotasthane, S.A. Shah, T. Habib, S. Liu, J.L. Lutkenhaus, pH, nanosheet concentration, and antioxidant affect the oxidation of Ti3C2Tx and Ti2CTx MXene dispersions, Adv. Mater. Interfaces (2020) 2000845.
[55] V. Natu, J.L. Hart, M. Sokol, H. Chiang, M.L. Taheri, M.W. Barsoum, Edge capping of 2D-MXene sheets with polyanionic salts to mitigate oxidation in aqueous colloidal suspensions, Angew. Chem. Int. 58 (2019) 12655–12660.
[56] K.C. Mutyala, H. Singh, R. Evans, G. Doll, Deposition, characterization, and performance of tribological coatings on spherical rolling elements, Surf. Coating. Technol. 284 (2015) 302–309.
[57] K.C. Mutyala, H. Singh, R. Evans, G. Doll, Effect of diamond-like carbon coatings on ball bearing performance in normal, oil-starved, and debris-damaged conditions, Tribol. Trans. 59 (2016) 1039–1047.
[58] K. Li, X. Wang, X. Wang, M. Liang, V. Nicolosi, Y. Xu, Y. Gogotsi, All-pseudocapacitive asymmetric MXene-carbon-conducting polymer supercapacitors, Nanomater. Energy 75 (2020) 104971.
[59] T. Hu, M. Hu, Z. Li, H. Zhang, C. Zhang, J. Wang, X. Wang, Interlayer coupling in two-dimensional titanium carbide MXenes, Phys. Chem. Chem. Phys. 18 (2016) 20256–20260.
[60] C. Glynn, O. Lotty, W. McSweeney, J.D. Holmes, C. O'Dwyer, Raman scattering spectroscopy of metal-assisted chemically etched rough Si nanowires, ECS Trans 35 (2011) 73–86.
[61] T. Zhou, C. Wu, Y. Wang, A.P. Tomsia, M. Li, E. Saiz, S. Fang, R.H. Baughman, L. Jiang, Q. Cheng, Super-tough MXene-functionalized graphene sheets, Nat. Commun. 11 (2020) 1–11.
[62] X. Yin, F. Wu, X. Chen, J. Xu, P. Wu, J. Li, C. Zhang, J. Luo, Graphene-induced reconstruction of the sliding interface assisting the improved lubricity of various tribo-couples, Mater. Des. 191 (2020) 108661.
[63] J. Archard, Contact and rubbing of flat surfaces, J. Appl. Phys. 24 (1953) 981–988.
[64] K.C. Mutyala, Y.A. Wu, A. Erdemir, A.V. Sumant, Graphene-MoS_2 ensembles to reduce friction and wear in DLC-Steel contacts, Carbon 146 (2019) 524–527.